

Determining the mass for an ultralight gravitino at LHC

K. Hamaguchi¹, S. Shirai¹ and T. T. Yanagida^{1,2}

¹ *Department of Physics, University of Tokyo,
Tokyo 113-0033, Japan*

² *Institute for the Physics and Mathematics of the Universe, University of Tokyo,
Chiba 277-8568, Japan*

Abstract

In supersymmetric (SUSY) models with the gravitino being the lightest SUSY particle (LSP), the SUSY breaking scale (i.e., the gravitino mass) could be determined by measuring the lifetime of the next-to-lightest SUSY particle (NLSP). However, for an ultralight gravitino of mass of $\mathcal{O}(1)$ eV, which is favored cosmologically, the determination of the SUSY breaking scale, or the gravitino mass, is difficult because the NLSP decay length is too short to be measured directly. Recently we proposed a new determination of the gravitino mass by measuring a branching fraction of two decay modes of sleptons. In this paper, we investigate the prospects for determining the gravitino mass at LHC. For demonstration we take some explicit gauge-mediation models and show that the gravitino mass can be determined with an accuracy of a few 10% for an integrated luminosity $10 - 100 \text{ fb}^{-1}$.

1 Introduction

The presence of a gravitino is the most fundamental prediction in supergravity [1] and its mass $m_{3/2}$ is an important parameter to determine the supersymmetry (SUSY)-breaking scale. The gravitino mass is predicted in a wide-range region, $m_{3/2} = 0.1 \text{ eV} - 100 \text{ TeV}$, depending on mediation mechanisms of the SUSY breaking to the SUSY standard-model (SSM) sector. The lowest mass region, $m_{3/2} = 0.1 \text{ eV} - 10 \text{ eV}$, is very interesting in particular, since there is no astrophysical and cosmological gravitino problem at all in this mass region [2]. If it is the case, the gravitino is the lightest SUSY particle (LSP), and the next-to-lightest SUSY particle (NLSP) decays into the gravitino inside detectors if it is produced at collider experiments. Therefore, we may have a signal for the NLSP decay into the gravitino at future collider experiments such as LHC. Furthermore, we may determine the gravitino mass from the mass and lifetime of the NLSP. However, for a light gravitino of mass $m_{3/2} \lesssim 10 \text{ eV}$ the NLSP lifetime is very short; for instance, the decay length is given by $c\tau_{\text{NLSP}} \simeq 0.55 \mu\text{m}(m_{3/2}/1 \text{ eV})^2(m_{\text{NLSP}}/200 \text{ GeV})^{-5}$ for a slepton NLSP, which is difficult to measure at collider experiments.

In a recent article [3], we proposed a new method to determine the gravitino mass (i.e., the SUSY-breaking scale) for a very light gravitino, by comparing the branching fractions of two decay modes of sleptons, $\tilde{\ell}_1 \rightarrow \tilde{\tau}_1 + \tau + \ell$ and $\tilde{\ell}_1 \rightarrow \ell + \tilde{G}_{3/2}$, instead of using the lifetime of the NLSP. (In this proposal we assume that the NLSP is the lighter stau $\tilde{\tau}_1$. $\tilde{\ell}_1$ denotes the lighter smuon or selectron, ℓ is μ or e , and $\tilde{G}_{3/2}$ is the gravitino.) However, we did not examine if this method works at LHC. The purpose of this paper is to show that the above method to determine the gravitino mass is indeed effective at LHC for a certain parameter region of the SUSY-particle spectrum. To demonstrate our point, we adopt simple gauge-mediated SUSY breaking (GMSB) models [4] in this paper. However, our mechanism for the determination of the gravitino mass is applicable to any gauge-mediation model as long as sleptons are the lightest next to the gravitino LSP and $m_{3/2} \lesssim 10 \text{ eV}$.

2 Measurement of the branching fraction for the slepton decays

In this section we explain the basic idea of our method. We assume that the NLSP is the lighter stau $\tilde{\tau}_1$, and the lighter smuon and selectron (collectively denoted by $\tilde{\ell}_1$) are heavier than the stau but lighter than the lightest neutralino $\tilde{\chi}_1^0$, $m_{\tilde{\tau}_1} < m_{\tilde{\ell}_1} < m_{\tilde{\chi}_1^0}$. In this case, $\tilde{\ell}_1$ have two dominant decay modes. One is the decay into the gravitino, and its decay rate is related to the gravitino mass:

$$\Gamma_{2\text{-body}} = \frac{m_{\tilde{\ell}_1}^5}{48\pi M_P^2 m_{3/2}^2} = 0.035\text{eV} \left(\frac{m_{\tilde{\ell}_1}}{200 \text{ GeV}} \right)^5 \left(\frac{m_{3/2}}{1 \text{ eV}} \right)^{-2}, \quad (1)$$

where $M_P = 2.44 \times 10^{18}$ GeV is the reduced Planck mass. The other decay mode is the three-body decay into the lighter stau, $\tilde{\ell}_1 \rightarrow \tilde{\tau}_1^\pm \tau^\mp \ell$. As pointed out in the previous work [3], if one can observe both of these decay modes, the gravitino mass can be determined. This is because the gravitino mass is written as

$$m_{3/2}^2 = \frac{m_{\tilde{\ell}_1}^5}{48\pi M_P^2} \left(\frac{\Gamma_{3\text{-body}}}{\Gamma_{2\text{-body}}} \right) \frac{1}{\Gamma_{3\text{-body}}}, \quad (2)$$

and $\Gamma_{3\text{-body}}$ is calculable once relevant SUSY particles' masses are known. Thus, we may derive the gravitino mass $m_{3/2}$ by measuring the branching fraction $\Gamma_{3\text{-body}}/\Gamma_{2\text{-body}}$.

Here we should comment on the measurement of the three-body decay rate $\Gamma_{3\text{-body}}$. In principle, $\Gamma_{3\text{-body}}$ depends on various SUSY parameters. However, in most of GMSB models with a light gravitino ($m_{3/2} = \mathcal{O}(1)$ eV), the lighter stau, smuon and selectron are approximately right handed sleptons, $\tilde{\tau}_1 \sim \tilde{\tau}_R, \tilde{\ell}_1 \sim \tilde{\ell}_R$, and the lightest neutralino is almost bino, $\tilde{\chi}_1^0 \sim \tilde{B}$. Therefore, we assume it is the case in the following discussion. Under those approximations, the three-body decay rate is given by [5]

$$\Gamma_{3\text{-body}} \simeq m_{\tilde{\ell}_R} \frac{1}{8\pi} \frac{\alpha_{\text{EM}}}{\cos^2 \theta_W} \int_0^{1-(r_\tau+r_{\tilde{\tau}})^2} dx x (1-x+r_\tau^2-r_{\tilde{\tau}}^2) (1-x+r_{\tilde{B}}^2) \times \frac{x \sqrt{(1-x)^2+r_\tau^2+r_{\tilde{\tau}}^2-2(1-x)r_\tau^2-2(1-x)r_{\tilde{\tau}}^2-2r_\tau^2r_{\tilde{\tau}}^2}}{(1-x)^2(r_{\tilde{B}}^2-1+x)^2}, \quad (3)$$

where $r_{\tilde{B}} = m_{\tilde{\chi}_1^0}/m_{\tilde{\ell}_R}, r_{\tilde{\tau}} = m_{\tilde{\tau}_1}/m_{\tilde{\ell}_R}, r_\tau = m_\tau/m_{\tilde{\ell}_R}$, and the lepton masses m_μ and m_e have been neglected. Here, we have defined $\Gamma_{3\text{-body}} = \Gamma(\tilde{\ell}_R \rightarrow \tilde{\tau}_1^+ \tau^- \ell) + \Gamma(\tilde{\ell}_R \rightarrow \tilde{\tau}_1^- \tau^+ \ell)$. We have checked that the approximation Eq.(3) is quite good and we can reproduce the

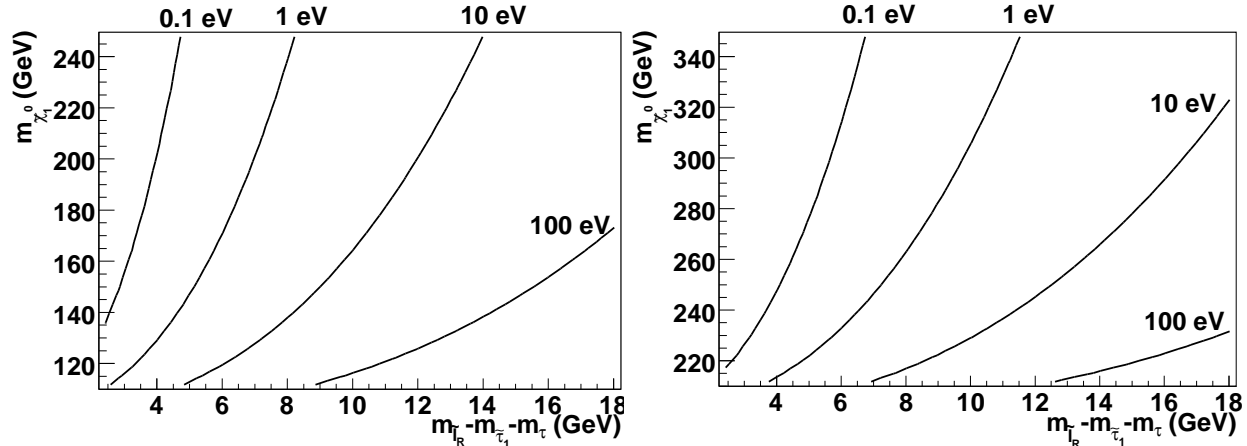


Figure 1: The contour plot of $\Gamma_{3\text{-body}}$. The left-side figure is for $m_{\tilde{\ell}_R} = 100$ GeV, and the right-side is for $m_{\tilde{\ell}_R} = 200$ GeV. The contour parameter is (0.1, 1, 10, 100) eV from left to right.

true $\Gamma_{3\text{-body}}$ with an accuracy of factor 30% via the approximation Eq.(3) for simple GMSB models explained in the next section. Therefore, by measuring the three masses $m_{\tilde{\chi}_1^0}$, $m_{\tilde{\ell}_R}$, and $m_{\tilde{\tau}_1}$, one can estimate the $\Gamma_{3\text{-body}}$ with a good accuracy. Contour plots of $\Gamma_{3\text{-body}}$ calculated by Eq.(3) is shown in Fig.1. Comparing them with Eq.(1), one can see that the two-body decay rates $\Gamma_{2\text{-body}}$ are comparable to the three-body decay rates $\Gamma_{3\text{-body}}$ in a certain parameter space.

Let us consider how we can measure the branching fraction $\Gamma_{3\text{-body}}/\Gamma_{2\text{-body}}$ at LHC. Comparing the three-body decay

$$\tilde{\ell}_R \rightarrow \ell + \tau(\text{soft}) + \tilde{\tau}_1 \rightarrow \ell + \tau(\text{soft}) + \tau + \tilde{G}_{3/2}, \quad (4)$$

with the two-body decay

$$\tilde{\ell}_R \rightarrow \ell + \tilde{G}_{3/2}, \quad (5)$$

we can see that the three-body decay accompanies a hard tau. Thus, as $\Gamma_{3\text{-body}}/\Gamma_{2\text{-body}}$ is larger, the number of taus produced in SUSY-like events becomes larger. Therefore, one may think that the branching fraction can be estimated by counting the excess of the number of hard taus in SUSY-like events. However, this method is troublesome because of the difficulty of tau-identification and the enormous backgrounds.

Here, we propose an alternative experimental method to measure the branching fraction $\Gamma_{3\text{-body}}/\Gamma_{2\text{-body}}$. At LHC, $\tilde{\ell}_R$ are likely to be produced through $\tilde{\chi}_1^0$'s decays. Thus,

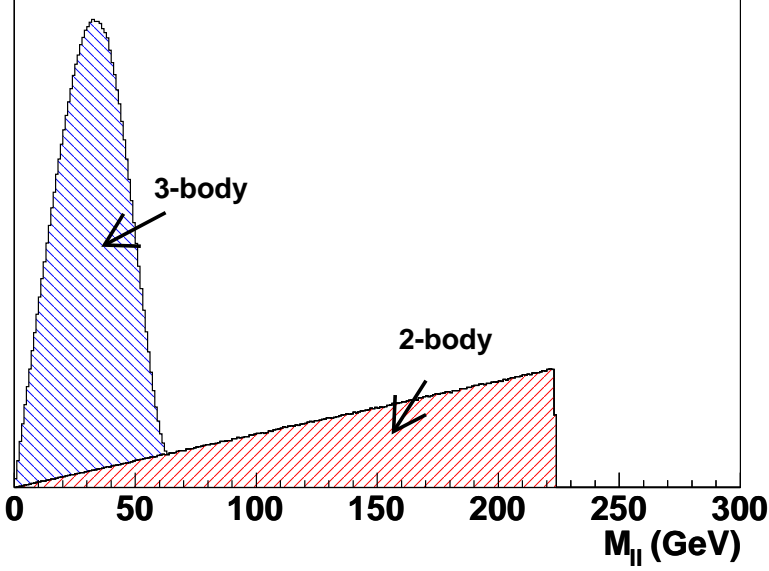


Figure 2: The $M_{\ell^+\ell^-}$ distribution. Here we set $m_{\tilde{\tau}_1} = 190$ GeV, $m_{\tilde{\ell}_R} = 200$ GeV, $m_{\tilde{B}} = 300$ GeV and $m_{3/2} = 1$ eV. The $M_{\ell^+\ell^-}$ distribution from the 2-body decay have an endpoint at $M_2^{\max} = \sqrt{m_{\tilde{B}}^2 - m_{\tilde{\ell}_R}^2} = 224$ GeV, and 3-body at $M_3^{\max} = \sqrt{m_{\tilde{B}}^2 - m_{\tilde{\ell}_R}^2} \sqrt{1 - (m_{\tau} + m_{\tilde{\tau}_1})^2 / m_{\tilde{\ell}_R}^2} = 63$ GeV. In this case, $\Gamma_{3\text{-body}} / \Gamma_{2\text{-body}} = 1.23$.

we consider the two decay chains, $\tilde{\chi}_1^0 \rightarrow \ell^\pm \tilde{\ell}_R^\mp \rightarrow \ell^\pm \ell^\mp \tilde{G}_{3/2}$ and $\tilde{\chi}_1^0 \rightarrow \ell^\pm \tilde{\ell}_R^\mp \rightarrow \ell^\pm \ell^\mp \tau \tilde{\tau}_1$. The dilepton invariant mass from the former chain has distribution with a sharp edge at $M_{\ell^+\ell^-} = \sqrt{m_{\tilde{\chi}_1^0}^2 - m_{\tilde{\ell}_R}^2}$. On the other hand, for the latter case the dilepton mass distribution has a peak which has an endpoint at $M_{\ell^+\ell^-} = \sqrt{m_{\tilde{\chi}_1^0}^2 - m_{\tilde{\ell}_R}^2} \sqrt{1 - (m_{\tau} + m_{\tilde{\tau}_1})^2 / m_{\tilde{\ell}_R}^2}$. An example of the dilepton mass distribution is shown Fig.2. From the ratio of these two peaks' areas, we estimate $\Gamma_{3\text{-body}} / \Gamma_{2\text{-body}}$.

We should note that the latter endpoint is crucial to determine the mass difference $\Delta m = m_{\tilde{\ell}_R} - (m_{\tau} + m_{\tilde{\tau}_1})$, which is one of the most important parameters for the calculation of $\Gamma_{3\text{-body}}$ (see Fig. 1). We also note that there are little background for the signal by virtue of the flavor subtraction technique, $e^+e^- + \mu^+\mu^- - e^\pm\mu^\mp$, where each dilepton represents the final-state one and the sign between each dilepton event defines if the event is added or subtracted when booked in the histogram.

Table 1: GMSB parameters of the models.

Point	Λ (TeV)	M (TeV)	N	$\tan\beta$	$\text{sgn}\mu$	C_{grav}
SPS7	40	80	3	15	+	1
Model1	40	80	3	13	+	1
Model2	40	80	3	10	+	5

3 Gauge-mediation models

We consider a simple gauge-mediation model, where a SUSY breaking field S couples to N pairs of messenger chiral superfields, ψ and $\bar{\psi}$, which transform as $\mathbf{5}$ and $\mathbf{5}^*$ under the $SU(5)_{\text{GUT}}$: $W = k\psi\bar{\psi}S$. The S field develops a vacuum expectation value $k\langle S \rangle = M + \theta^2 F$, where M is the messenger mass. With these conditions the low-energy spectrum of the SUSY particles including the gravitino mass are determined by 6 parameters, $\Lambda = F/M$, M , N , $\tan\beta$, $\text{sgn}(\mu) = \pm 1$, and C_{grav} [4]. The gaugino masses are generated from loop diagrams of the messengers and are given by, at the one-loop level,

$$m_a = \frac{N\alpha_a}{4\pi}\Lambda \quad (a = 1, 2, 3), \quad (6)$$

where $\Lambda = F/M$ and $\alpha_1 = 5\alpha_{\text{EM}}/(3\cos^2\theta_W)$. Scalar masses, at the two loop level, are given by

$$m_{\phi_i}^2 = 2N\Lambda^2 \sum_a \left(\frac{\alpha_a}{4\pi}\right)^2 C_a(i), \quad (7)$$

where $C_a(i)$ are Casimir invariants for the particle ϕ_i ($C_1(i) = 3Y_i^2/5$). Here, we have omitted the higher order terms in an expansion in F/M^2 . The above gaugino and scalar masses are given at the messenger scale, and the physical masses should be obtained by solving the renormalization group equations. Finally, the gravitino mass is given by $m_{3/2} = (C_{grav}/\sqrt{3})(F/M_P)$.

For numerical analyses in the next section, we choose a few model points: one is the Snowmass point SPS7 [6], and we also take two other model points to demonstrate the dependence on the model parameters. The GMSB parameters of those models are shown in Table. 1. In Fig.3, those model points are shown in $(m_{3/2}, \tan\beta)$ -plane, together with contour plots of $\Gamma_{3\text{-body}}/\Gamma_{2\text{-body}}$. The full mass spectrum of the models are shown in Table. 2.¹

¹Here, the mass spectrum is calculated by ISAJET 7.67 [8], and used in the event generation in the

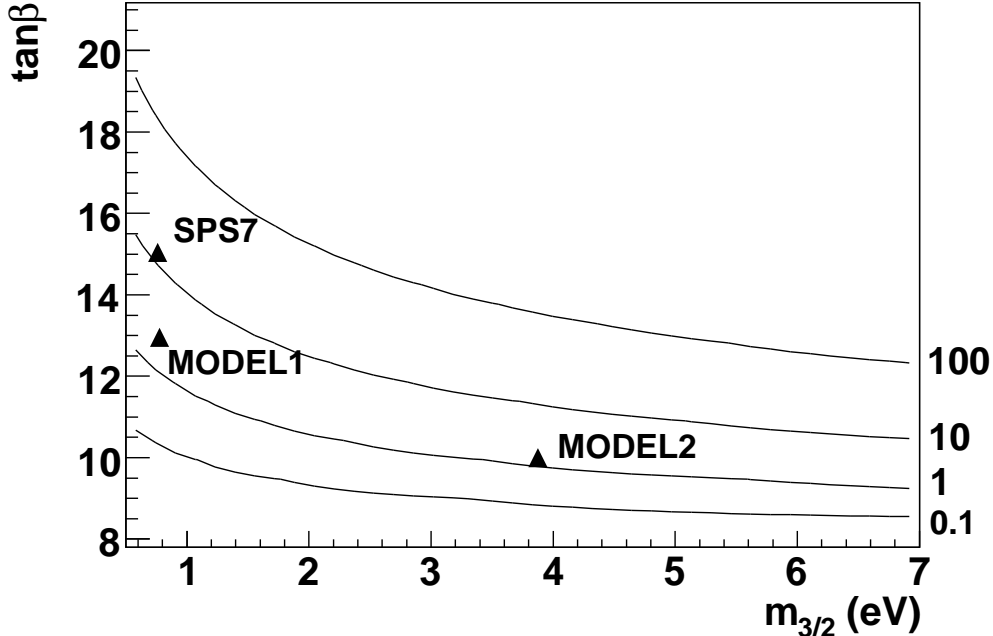


Figure 3: The contour plot of $\Gamma_{3\text{-body}}/\Gamma_{2\text{-body}}$ in the $(m_{3/2}, \tan\beta)$ plane. We set $\Lambda = 40$ TeV, $M = 80$ TeV, $N = 3$, $\text{sgn}(\mu) = +$. In this figure, we calculate the mass spectrum and the decay rates by the program SOFTSUSY [7] as in Ref. [3]. The marks represent the model points we discuss in the text.

4 Determination of the gravitino mass at LHC

In this section we show that the gravitino mass can indeed be determined at LHC, by taking SPS7, model 1 and 2 as examples. In all analyses we use an event generator HERWIG 6.5 [9].

Let us first consider the parton-level signatures of signal events. In Fig.4, the distribution of the opposite charge dilepton invariant mass $M_{\ell\ell}$ is shown for the model 1.² Here the flavor-subtraction in the final state, $e^+e^- + \mu^+\mu^- - e^\pm\mu^\mp$, is adopted. As expected, one can clearly see the two peaks from two- and three-body decays of the slepton.

following section.

²It seems that the matrix element of the three-body decay $\tilde{\ell}_R \rightarrow \tilde{\tau}_1^\pm \tau^\mp \ell$ is not implemented in Herwig (i.e., the matrix element is taken to be constant). Note that the end point of $M_{\ell\ell}$ distribution from the three-body decay and the branching fraction is unchanged even if one takes it into account, and therefore only the shape of the first peak is affected. One may wonder that the reduction factor Eq. (8) due to the soft-lepton cut $P_T > 6$ GeV is affected by this approximation, but we have checked that the inclusion of the correct matrix element does not change the result much.

Table 2: Mass spectrum

Particle	SPS7	Model1	Model2	Particle	SPS7	Model1	Model2
\tilde{g}	952.3	952.1	952.4	$\tilde{G}_{3/2}$	0.77 eV	0.77 eV	3.85 eV
\tilde{u}_L	902.1	902.1	902.2	\tilde{u}_R	872.8	872.7	872.9
\tilde{d}_L	905.8	905.8	905.8	\tilde{d}_R	871.3	871.3	871.4
\tilde{b}_2	876.1	875.9	875.5	\tilde{b}_1	863.8	865.0	866.9
\tilde{t}_2	895.8	896.1	896.6	\tilde{t}_1	811.1	810.9	810.2
$\tilde{\nu}$	251.1	251.1	251.1	$\tilde{\nu}_\tau$	250.6	250.7	250.9
\tilde{e}_L	267.5	267.5	267.5	\tilde{e}_R	129.1	129.1	129.0
$\tilde{\tau}_2$	268.8	268.5	268.0	$\tilde{\tau}_1$	122.3	124.0	126.0
$\tilde{\chi}_1^0$	160.1	160.0	159.8	$\tilde{\chi}_2^0$	274.9	275.0	275.6
$\tilde{\chi}_3^0$	325.0	325.6	327.6	$\tilde{\chi}_4^0$	388.8	389.3	390.9
$\tilde{\chi}_1^\pm$	269.4	269.1	268.9	$\tilde{\chi}_2^\pm$	391.2	392.0	394.0
h^0	113.6	113.4	112.8	H^0	389.7	393.5	400.1
A	389.5	393.2	399.5	H^\pm	397.8	401.4	407.5

However, events are subject, at LHC, to various cuts from experimental constraints and from reducing the backgrounds, and hence the real event distribution may not necessarily follow the ideal one. In fact, in many cases, the reduction factor

$$R = \frac{\# \text{ of dileptons with the cuts}}{\# \text{ of dileptons without any cuts}} \quad (8)$$

tends to be non-negligible. If the reduction factor differs between for two-body and for three-body decay events, the $\Gamma_{3\text{-body}}/\Gamma_{2\text{-body}}$ is affected by the cuts.

In fact, we require that

- the dilepton mass is formed only if one of the two leptons has $P_T \geq 20$ GeV, $|\eta| < 2.5$ and the other has $P_T \geq 6$ GeV,³ $|\eta| < 2.5$,

where P_T and η denotes the transverse momentum and the pseudorapidity, respectively. This requirement affects the ratio $\Gamma_{3\text{-body}}/\Gamma_{2\text{-body}}$. Because of the small difference between $m_{\tilde{\tau}_1}$ and $m_{\tilde{\ell}_R}$, the lepton from the three-body decay is typically soft. Therefore, the first peak from the three-body decay shrinks by the P_T cuts. The distribution of $M_{\ell\ell}$ after the cuts is also shown in Fig.4, by the hatched histogram. As can be seen, only the events of three-body decay is substantially reduced.

³We have checked that our method works even if a harder cut $P_T > 10$ GeV is taken.

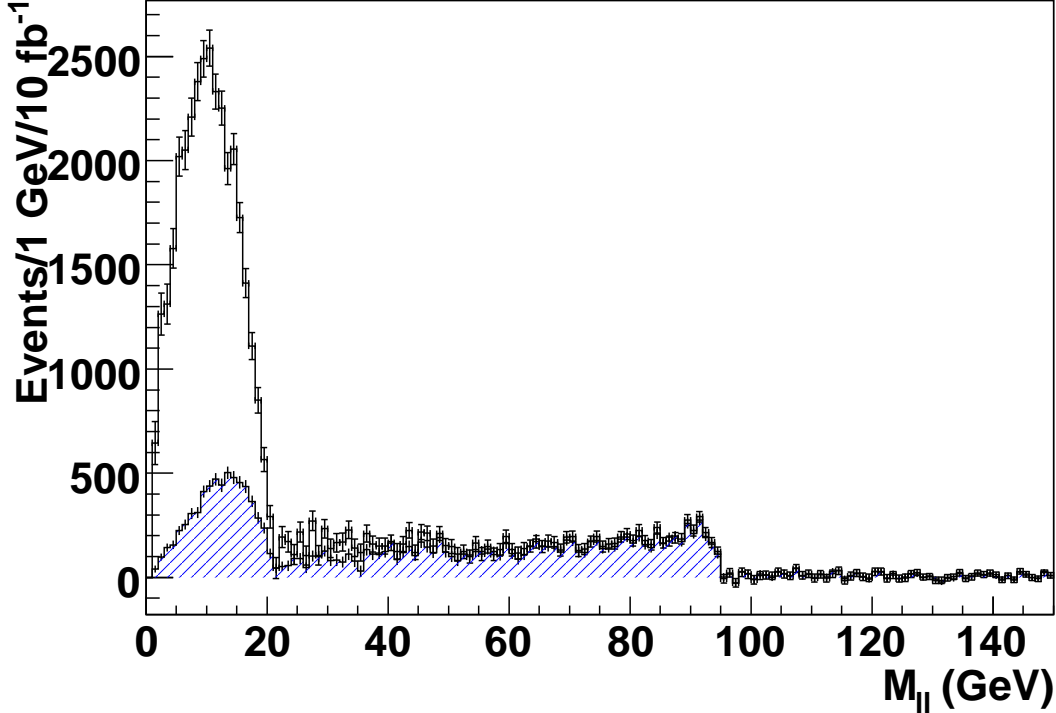


Figure 4: The distribution of $M_{\ell\ell}$. As expected, we can see two peaks of endpoints at $M_3^{\max} = 21.3$ GeV and $M_2^{\max} = 94.5$ GeV. The hatched histogram shows the distribution after the cuts on the lepton P_T . The peak from the three-body decay is clearly shown in the region of $M_{\ell\ell} \lesssim 20$ GeV, and in $60 \text{ GeV} \lesssim M_{\ell\ell} \lesssim 90$ GeV one can see the characteristic shape of $M_{\ell\ell}$ distribution from two-body decay. Note also that in $M_{\ell\ell} \lesssim 60$ GeV there is another tiny peak which comes from the decay chain of the next to lightest neutralino, $\tilde{\chi}_2^0 \rightarrow \ell^\pm \tilde{\ell}_R^\mp \rightarrow \ell^\pm \ell^\mp \tilde{\tau}_1 \tau$, which has an endpoint at $\sqrt{m_{\tilde{\chi}_2^0}^2 - m_{\tilde{\ell}_R}^2} \sqrt{1 - (m_{\tilde{\tau}_1} + m_\tau)^2 / m_{\tilde{\ell}_R}^2} = 54.7$ GeV.

We have found that there is a correlation between the ratio of two peaks' endpoints $M_3^{\max}/M_2^{\max} = \sqrt{1 - (m_{\tilde{\tau}_1} + m_\tau)^2 / m_{\tilde{\ell}_R}^2}$ and the reduction factor R_3 of the three-body decay as shown in Fig.5. Here we have adopted various parameter regions in the simple GMSB model described in Sec. 3. We will use this correlation to reproduce the true branching fraction.

Now let us discuss experimental signatures for each models in turn. For a detector simulation, we use a package AcerDET-1.0 [10]. We select events by the following requirements;

- at least four jets with $P_T \geq 25$ GeV, where τ -jets are excluded.

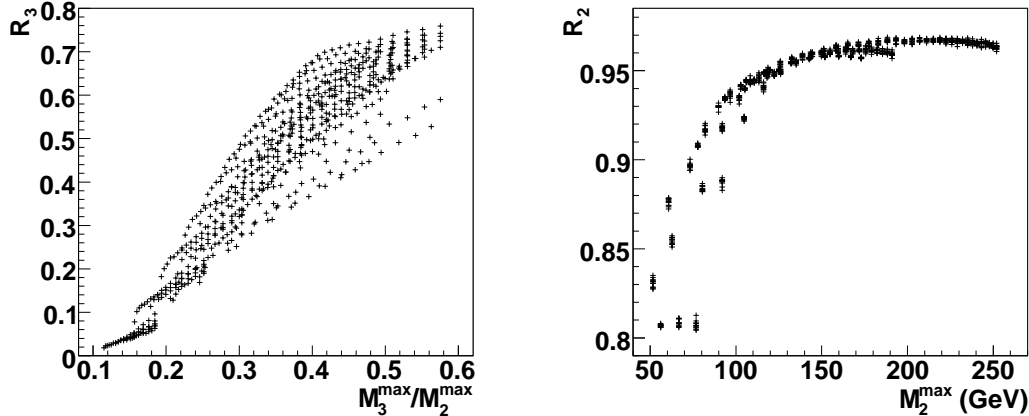


Figure 5: The correlation between M_3^{\max}/M_2^{\max} and R_3 for three-body decay (left) and M_2^{\max} and R_2 for two-body decay (right). We have adopted simple GMSB models with parameters $(N, \Lambda, M, \tan \beta) = (\{3, 4, 5\}, 30 \text{ TeV}, 60 \text{ TeV}, 15)$ and $(\{3, 4, 5\}, 40 \text{ TeV}, 80 \text{ TeV}, 18)$. In each model, we further vary the value of $m_{\tilde{\tau}_1}$ and $m_{\tilde{\ell}_R}$ as free parameters, imposing $m_{\tilde{\chi}_1^0} > m_{\tilde{\ell}_R} + 10 \text{ GeV}$ and $m_{\tilde{\ell}_R} > 100 \text{ GeV}$.

- missing transverse momentum $P_{T,\text{miss}} \geq 100 \text{ GeV}$.
- $M_{\text{eff}} \geq 500 \text{ GeV}$, where

$$M_{\text{eff}} = \sum_{\text{jets}(\neq \tau)}^4 P_{T_j} + P_{T,\text{miss}}. \quad (9)$$

- two leptons with $P_T \geq 20 \text{ GeV}$ and $|\eta| < 2.5$.

We have checked that the first three cuts reduce the two decay chains $\tilde{\chi}_1^0 \rightarrow \ell^\pm \tilde{\ell}_R^\mp \rightarrow \ell^\pm \ell^\mp \tilde{G}_{3/2}$ and $\tilde{\chi}_1^0 \rightarrow \ell^\pm \tilde{\ell}_R^\mp \rightarrow \ell^\pm \ell^\mp \tau \tilde{\tau}_1$ almost equally and hence the ratio of the number of dileptons from the two- and three-body decay chains remains almost unchanged. The cut of two high P_T leptons slightly change the ratio, but not very much.⁴ We then form the dilepton invariant mass for opposite charge leptons which satisfy $P_T \geq 20 \text{ GeV}$, $|\eta| < 2.5$ and $P_T \geq 6 \text{ GeV}$, $|\eta| < 2.5$.⁵ As discussed above, this last requirement affect the ratio of number of events, and hence the reduction factor R should be taken into account.

⁴ In fact, when a pair of sparticle cascades in a SUSY event end up with two decay chains where one is $\dots \rightarrow \tilde{\chi}_1^0 \rightarrow \tilde{\tau}_1 \tau$ and the other is $\dots \rightarrow \tilde{\chi}_1^0 \rightarrow \tilde{\ell}_R \ell \rightarrow \tilde{\tau}_1 \tau \ell(\text{soft})\ell$, this event is likely to be cut by this requirement of two high P_T leptons. This reduces the number of three-body decay events, and decreases the resultant gravitino mass by about 20%.

⁵ In our analysis, we do not take into account of miss-identification of soft leptons.

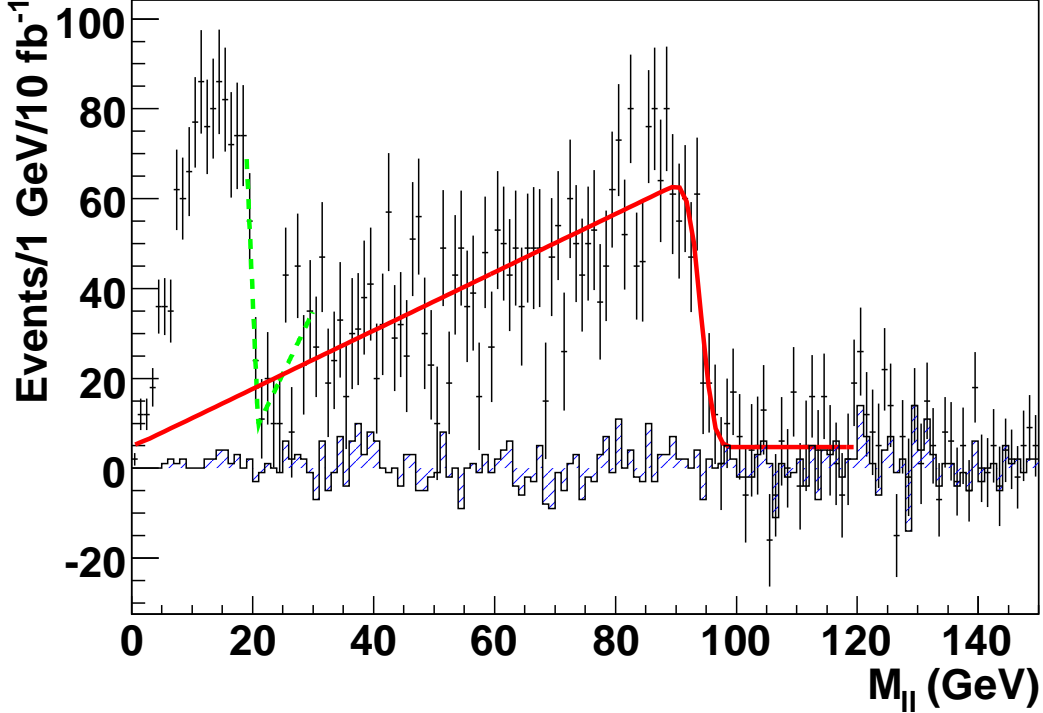


Figure 6: The distribution of $M_{\ell\ell}$ for the model 1. The hatched histogram is standard model background mainly from $t\bar{t}$ production

4.1 The model 1

In Fig.6, the flavor subtracted ($e^+e^- + \mu^+\mu^- - e^\pm\mu^\mp$) distribution of the dilepton mass after the cuts is shown for the model 1. Here, we have assumed an integrated luminosity $\mathcal{L} = 10 \text{ fb}^{-1}$. We also show the main background from the $t\bar{t}$ events. We fit the data over $70 \text{ GeV} < M_{\ell\ell} < 120 \text{ GeV}$ via a line smeared with a Gaussian, and obtain

$$M_2^{\max} = 94.1 \pm 0.5 \text{ GeV}. \quad (10)$$

To find M_3^{\max} , we fit the data with a function

$$h(x) = a(x - M)\theta(-x + M) + bx + c, \quad (11)$$

over $19 \text{ GeV} < M_{\ell\ell} < 30 \text{ GeV}$, where $x = M_{\ell\ell}$. Then we get

$$M_3^{\max} = 21.1 \pm 1 \text{ GeV}. \quad (12)$$

The estimation of the error is done by 'eye'. Then, we find that the number of dileptons for the two-body decay is $N_2 = 2876 \pm 201$, and $N_3 = 958 \pm 51$ for the three-body decay.^{6,7} From Fig.5, we estimate the reduction factor of the three-body decay is $R_3 = 0.20 \pm 0.05$, and those for the two-body decay $R_2 = 0.90 \pm 0.02$. Here, the errors are systematic. Then, we find⁸

$$\frac{\Gamma_{3\text{-body}}}{\Gamma_{2\text{-body}}} = \frac{N_3 R_2}{N_2 R_3} = (1.50 \pm 0.15) \left(\frac{R_2}{0.90}\right) \left(\frac{R_3}{0.20}\right)^{-1} \quad (13)$$

Suppose that we know $m_{\tilde{\ell}_R} = 129.1 \pm 0.5$ GeV which will be determined from additional observations like $m_{j\ell}$ and $m_{j\ell\ell}$ distributions [12]. We can then calculate the approximate $\Gamma_{3\text{-body}}$ from $m_{\tilde{\ell}_R}$, M_2^{\max} and M_3^{\max} , by using Eq.(3). In the present case, we obtain

$$\Gamma_{3\text{-body}} = 0.21_{-0.07}^{+0.09} \text{ eV} \quad (\text{the true value is } \Gamma_{3\text{-body}} = 0.22 \text{ eV}). \quad (14)$$

Combining Eq.(13) and (14) we derive the gravitino mass from Eq.(2) as

$$m_{3/2} = (0.53_{-0.10}^{+0.11}) \left(\frac{R_2}{0.90}\right)^{\frac{1}{2}} \left(\frac{R_3}{0.20}\right)^{-\frac{1}{2}} \text{ eV}. \quad (15)$$

This value is in a good agreement with the expected one $m_{3/2} = 0.77$ eV.

4.2 The model 2

In Fig.7, the flavor subtracted ($e^+e^- + \mu^+\mu^- - e^\pm\mu^\mp$) distribution of the dilepton mass after the cuts is shown for the model 2, for an integrated luminosity $\mathcal{L} = 100 \text{ fb}^{-1}$. We also show the main background from $t\bar{t}$ events. In this case, an integrated luminosity $\mathcal{L} = 100 \text{ fb}^{-1}$ would be necessary to determine the gravitino mass.

We fit the data over $70 \text{ GeV} < M_{\ell\ell} < 120 \text{ GeV}$ via a line smeared with a Gaussian and find $M_2^{\max} = 94.1 \pm 0.2$ GeV. Also, we fit over $9 \text{ GeV} < M_{\ell\ell} < 19 \text{ GeV}$ via $h(x)$ in Eq.(11) and find $M_3^{\max} = 13.2 \pm 3$ GeV. Then, we estimate $N_2 = 41627 \pm 1066$ and $N_3 = 1561 \pm 784$. We can see $R_3 = 0.04 \pm 0.02$, $R_2 = 0.90 \pm 0.02$ from Fig.5. Then, we obtain

$$\frac{\Gamma_{3\text{-body}}}{\Gamma_{2\text{-body}}} = \frac{N_3 R_2}{N_2 R_3} = (0.85 \pm 0.42) \left(\frac{R_2}{0.90}\right) \left(\frac{R_3}{0.04}\right)^{-1} \quad (16)$$

⁶ Here, those numbers are obtained by extrapolating the fitted line. It may be modified at lower $M_{\ell\ell}$ region depending on the detector performance (cf. [11]), but such an effect is small.

⁷ The estimation of N_3 could be affected by the contamination of the events from the decay of the second lightest neutralino $\tilde{\chi}_0^2$, but its effect is negligible (cf. Fig. 4).

⁸Here, the correlation between N_2 and N_3 is neglected for simplicity, taking those parameters to be independent.

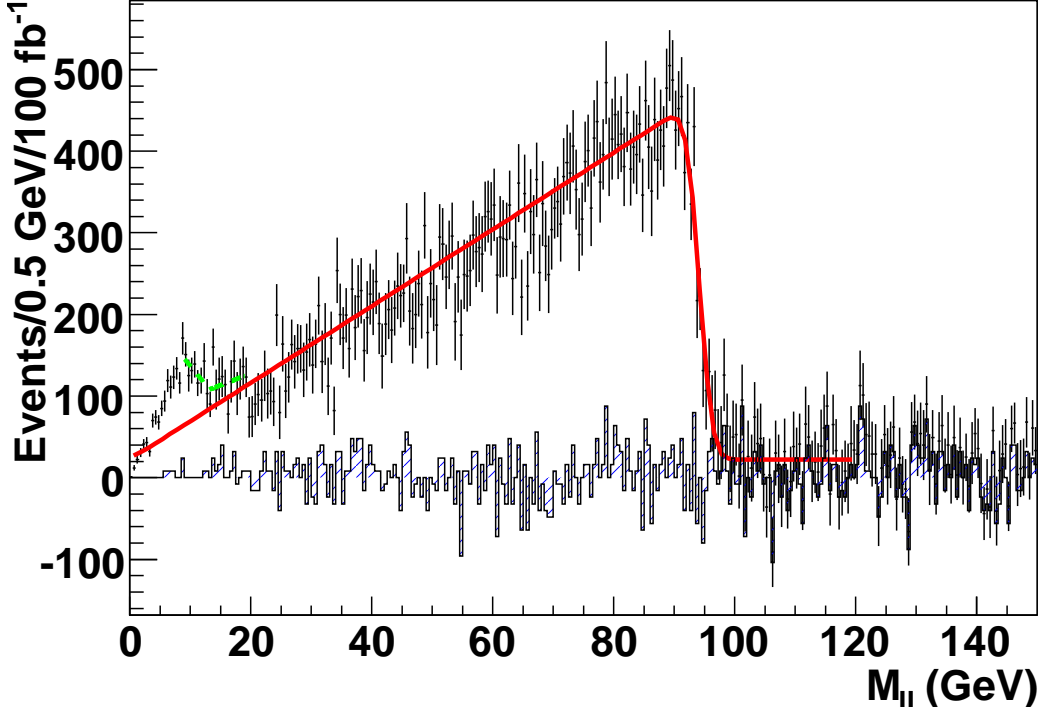


Figure 7: The distribution of $M_{\ell\ell}$ for the model 2. The hatched histogram is standard model background.

Supposing $m_{\tilde{\ell}_R} = 129.0 \pm 0.5$ GeV, we estimate

$$\Gamma_{3\text{-body}} = 0.006^{+0.021}_{-0.005} \text{eV} \quad (\text{the true value is } \Gamma_{3\text{-body}} = 0.006 \text{ eV}), \quad (17)$$

which leads to

$$m_{3/2} = (2.3^{+4.5}_{-1.4}) \left(\frac{R_2}{0.90}\right)^{\frac{1}{2}} \left(\frac{R_3}{0.04}\right)^{-\frac{1}{2}} \text{eV}. \quad (18)$$

The expected value is $m_{3/2} = 3.85$ eV.

4.3 The SPS7

In Fig.8, the flavor subtracted ($e^+e^- + \mu^+\mu^- - e^\pm\mu^\mp$) distribution of the dilepton mass after the cuts is shown for the SPS7 model point, for an integrated luminosity $\mathcal{L} = 100 \text{ fb}^{-1}$. We also show the main background from $t\bar{t}$ events.

We fit the data over $70 \text{ GeV} < M_{\ell\ell} < 120 \text{ GeV}$ via a line smeared with a Gaussian plus a peak from Z^0 -boson decays and find $M_2^{\text{max}} = 93.5 \pm 1.4$ GeV. Also we fit the data

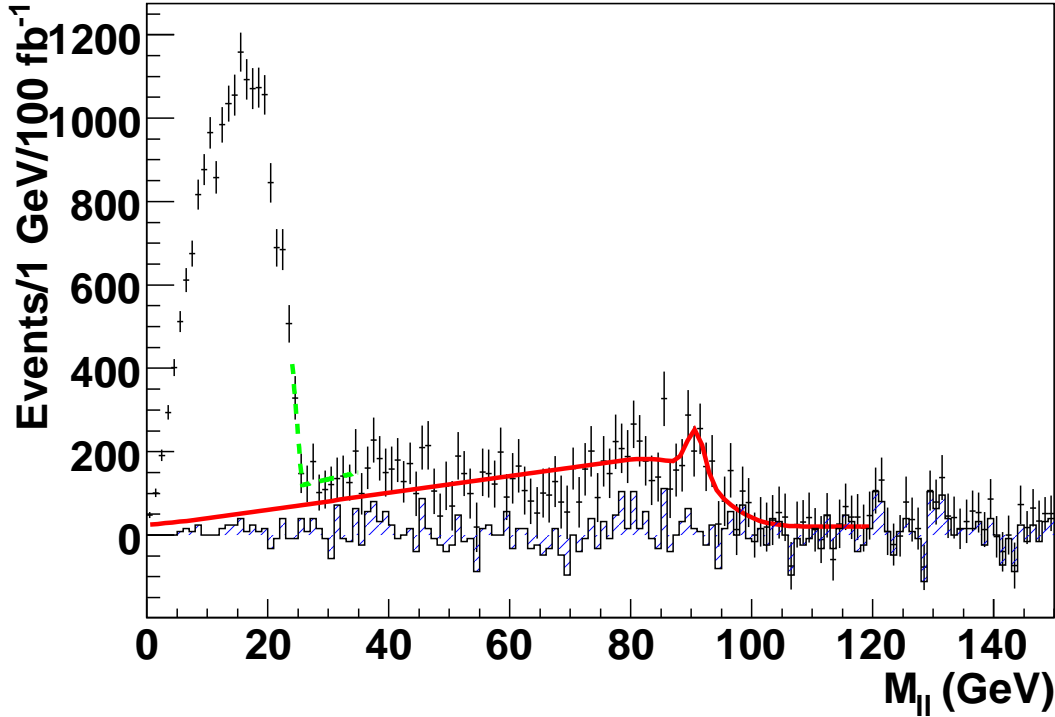


Figure 8: The distribution of $M_{\ell\ell}$ at SPS7. The hatched histogram is standard model background. The peak around 90 GeV is due to the Z^0 decays.

over $24 \text{ GeV} < M_{\ell\ell} < 35 \text{ GeV}$ via $h(x)$ in Eq.(11) and find $M_3^{\max} = 25.7 \pm 2 \text{ GeV}$. Then we estimate $N_2 = 8860 \pm 1281$ and $N_3 = 17265 \pm 498$. We can see $R_3 = 0.35 \pm 0.10$, $R_2 = 0.90 \pm 0.02$ from Fig.5. Thus, we obtain

$$\frac{\Gamma_{3\text{-body}}}{\Gamma_{2\text{-body}}} = \frac{N_3 R_2}{N_2 R_3} = (5.01 \pm 0.84) \left(\frac{R_2}{0.90}\right) \left(\frac{R_3}{0.35}\right)^{-1} \quad (19)$$

Assuming that we know $m_{\tilde{\ell}_R} = 129.1 \pm 0.5 \text{ GeV}$, we estimate

$$\Gamma_{3\text{-body}} = 1.16_{-0.59}^{+1.28} \text{ eV} \quad (\text{the true value is } \Gamma_{3\text{-body}} = 1.11 \text{ eV}), \quad (20)$$

which leads to

$$m_{3/2} = (0.41_{-0.12}^{+0.17}) \left(\frac{R_2}{0.90}\right)^{\frac{1}{2}} \left(\frac{R_3}{0.35}\right)^{-\frac{1}{2}} \text{ eV}. \quad (21)$$

The expected value is $m_{3/2} = 0.77 \text{ eV}$.

5 Conclusion and Discussion

We have investigated the prospects for determining the mass of an ultralight gravitino at LHC, by measuring the branching fraction of two decay modes of sleptons. We have performed detailed analyses by taking some specific GMSB models, and demonstrated that the proposed method can indeed work at LHC. Although we have taken simple GMSB models, our method works independently of details of GMSB models, as far as the two decay modes of sleptons are seen and the relevant mass parameters are all known.

So far in this paper, we have assumed that the missing particle is the gravitino LSP and discussed how to determine its mass by measuring the two decay modes of sleptons. Conversely, one may argue that, if the two characteristic peaks of two- and three-body decays of sleptons are simultaneously seen in the dilepton invariant mass distribution, they themselves suggest that the missing particle is not a neutralino but the gravitino LSP, and therefore the underlying model is a GMSB model. One can then perform analyses as presented in this paper and determine the gravitino mass, or equivalently the SUSY breaking scale, which will be one of the most important physics target after the discovery of SUSY.

Acknowledgement

We would like to thank the organizers of "LHC visiting program" at KEK, June 2007, especially M. M. Nojiri for the tutorials on the tools for high energy physics. We also thank S. Asai for discussions. The work by KH was supported by JSPS (18840012).

References

- [1] D. Z. Freedman, P. van Nieuwenhuizen and S. Ferrara, Phys. Rev. D **13** (1976) 3214; S. Deser and B. Zumino, Phys. Lett. B **62** (1976) 335.
- [2] H. Pagels and J. R. Primack, Phys. Rev. Lett. **48** (1982) 223; M. Viel, J. Lesgourgues, M. G. Haehnelt, S. Matarrese and A. Riotto, Phys. Rev. D **71** (2005) 063534 [arXiv:astro-ph/0501562].

- [3] K. Hamaguchi, S. Shirai and T. T. Yanagida, *Phys. Lett. B* **651** (2007) 44 [arXiv:0705.0219 [hep-ph]].
- [4] See for a review, G. F. Giudice and R. Rattazzi, *Phys. Rept.* **322** (1999) 419 [arXiv:hep-ph/9801271].
- [5] S. Ambrosanio, G. D. Kribs and S. P. Martin, *Nucl. Phys. B* **516** (1998) 55 [arXiv:hep-ph/9710217].
- [6] B. C. Allanach *et al.*, in *Proc. of the APS/DPF/DPB Summer Study on the Future of Particle Physics (Snowmass 2001)* ed. N. Graf, *In the Proceedings of APS / DPF / DPB Summer Study on the Future of Particle Physics (Snowmass 2001), Snowmass, Colorado, 30 Jun - 21 Jul 2001, pp P125* [arXiv:hep-ph/0202233].
- [7] B. C. Allanach, *Comput. Phys. Commun.* **143** (2002) 305 [arXiv:hep-ph/0104145].
- [8] F. E. Paige, S. D. Protopopescu, H. Baer and X. Tata, arXiv:hep-ph/0312045.
- [9] G. Marchesini, B. R. Webber, G. Abbiendi, I. G. Knowles, M. H. Seymour and L. Stanco, *Comput. Phys. Commun.* **67** (1992) 465;
G. Corcella *et al.*, *JHEP* **0101** (2001) 010 [arXiv:hep-ph/0011363];
G. Corcella *et al.*, arXiv:hep-ph/0210213.
- [10] E. Richter-Was, arXiv:hep-ph/0207355.
- [11] B. K. Gjelsten, D. J. Miller and P. Osland, *JHEP* **0412** (2004) 003 [arXiv:hep-ph/0410303].
- [12] I. Hinchliffe and F. E. Paige, *Phys. Rev. D* **60** (1999) 095002 [arXiv:hep-ph/9812233];
J. Sjolín, *Eur. Phys. J. direct C* **4** (2002) 11.